Fabrication of Mesoporous Silica Microtubules through the Self-Assembly Behavior of β-Cyclodextrin and Triton X-100 in Aqueous Solution

Qifang Lu, Dairong Chen,* and Xiuling Jiao

Department of Chemistry, Shandong University, Jinan 250100, P. R. China

Received January 23, 2005. Revised Manuscript Received June 13, 2005

Mesoporous silica microtubules were hydrothermally prepared with tetraethoxysilane (TEOS) as silica source and the supramolecular assembly of β-cyclodextrin and the nonionic surfactant Triton X-100 (TX-100) as the structure-directing agent. The products exhibit a well-developed tubular morphology with diameters between 0.8 and 2 μm, wall thicknesses of 0.2−1 μm, and lengths up to 10−25 μm. The morphology and mesoporous structure of the microtubules are preserved after calcination at 550 °C for 5 h, and their pore size and Brunauer−Emmett−Teller (BET) surface area are 2.3 nm and 847 m^2/g, respectively. The formation mechanism of mesoporous microtubules based on the bending of silica membranes is proposed to occur by a topological transformation.

Introduction

Much recent work has focused on developing new classes of inorganic materials with a hierarchical structure on at least two different length scales and well-defined macroscopic forms. Of all the hierarchical materials, mesoporous fibers have attracted the most attention, since they can serve as waveguides and as laser materials after doping with dyes.[1−4] Moreover, mesoporous tubules, hollow fibers with mesoporous structure, present a very high degree of structural particularity of hierarchical organization for their three different surfaces and so would have wide applications in nanotechnology, especially in catalysis, separation technology, biomaterials engineering, and fabrication of nanodevices.[5,6] For alignment and functionalization procedures, an anisotropic tubular morphology is certainly advantageous. The tubular mesoporous structures have prompted research into the physical and chemical properties of molecules confined in their inner nanospaces and eventually might lead to the mimicking of biological channels.[7] In addition, the modification of the properties either by filling or by coating tubules has been developed to fit particular application requirements.

Since the first report on the synthesis of MCM-41 hollow tubules from a membrane-to-tubule transformation in a high alkaline solution by Mou's group,[8,9] there have been a few investigations into preparing mesoporous silica tubules, and several methods have been proposed. Marlow et al. synthesized hollow silica fibers with the precursor molecules dissolved in an oil phase and surfactant molecules in a separate acidic aqueous phase.[10,11] Ozin and co-workers obtained mesoporous silica hollow helicoids of a hierarchical architecture. These hollow helicoids are comprised of 5 nm diameter channels that coil in the form of a micrometer scale tubular spiral,[12] and Shinkai et al. prepared mesoporous silica tubules using organic gel fibers as a template.[13] Mesoporous silica tubes or fibers were prepared using porous polycarbonate and Al_2O_3 membrane as templates.[14,15]

Although some success has been achieved, the synthesis of silica tubules with mesoporous structures still remains a challenge. There are still few synthetic methods, and moreover, the existing methods have some occasionality.

Herein, we describe a simple one-phase hydrothermal route to prepare mesoporous silica microtubules derived from supramolecular assemblies of β-cyclodextrins with nonionic surfactant TX-100. In this procedure, the morphologies and internal pore architectures of the mesoporous materials are

* Corresponding author. Phone: +86-531-88364280. Fax: +86-0531-88364281. E-mail: cdr@sdu.edu.cn.

(1) Wang, J.; Zhang, J.; Asoo, B. Y.; Stucky, G. D. *J. Am. Chem. Soc.* **2003**, *125*, 13966.
(2) (a) Schacht, S.; Huo, Q. S.; Voigt-Martin, I. G.; Stucky, G. D.; Schüth, F. *Science* **1996**, *273*, 768. (b) Huo, Q. S.; Zhao, D. Y.; Feng, J. L.; Weston, K.; Buratto, S. K.; Stucky, G. D.; Schacht, S.; Schüth, F. *Adv. Mater.* **1997**, *9*, 974. (c) Marlow, F.; Spliethoff, B.; Tesche, B.; Zhao, D. Y. *Adv. Mater.* **2000**, *12*, 961. (d) Kleitz, F.; Marlow, F.; Stucky, G. D.; Schüth, F. *Chem. Mater.* **2001**, *13*, 3587. (e) Marlow, F.; Leike, I.; Weidenthaler, C.; Lehmann, C. W.; Wilczok, U. *Adv. Mater.* **2001**, *13*, 307.
(3) Yang, P.; Zhao, D. Y.; Chmelka, B. F.; Stucky, G. D. *Chem. Mater.* **1998**, *10*, 2033.
(4) Yang, Z. L.; Niu, Z. W.; Cao, X. Y.; Yang, Z. Z.; Lu, Y. F.; Hu, Z. B.; Han, C. C. *Angew. Chem., Int. Ed.* **2003**, *42*, 4201.
(5) Kleitz, F.; Marlow, F.; Stucky, G. D.; Schüth, F. *Chem. Mater.* **2001**, *13*, 3587.
(6) Guo, C. W.; Cao, Y.; Xie, S. H.; Dai, W. L.; Fan, K. N. *Chem. Commun.* **2003**, 700.
(7) Jung, J. H.; Kobayashi, H.; van Bommel, K. J. C.; Shinkai, S.; Shimizu, T. *Chem. Mater.* **2002**, *14*, 1445.
(8) Lin, H. P.; Mou, C. Y. *Science* **1996**, *273*, 765.
(9) Lin, H. P.; Cheng, S.; Mou, C. Y. *Chem. Mater.* **1998**, *10*, 581.
(10) Kleitz, F.; Wilczok, U.; Schüth, F.; Marlow, F. *Phys. Chem. Chem. Phys.* **2001**, *3*, 3486.
(11) Marlow, F.; Kleitz, F. *Microporous Mesoporous Mater.* **2001**, *44*, 671.
(12) Yang, S. M.; Sokolov, I.; Coombs, N.; Kresge, C. T.; Ozin, G. A. *Adv. Mater.* **1999**, *11*, 1427.
(13) Ono, Y.; Nakashima, K.; Sano, M.; Kanekiyo, Y.; Inoue, K.; Hojo, H.; Shinkai, S. *Chem. Commun.* **1998**, 1477.
(14) Yang, Z.; Niu, Z.; Cao, X.; Yang, Z.; Lu, Y.; Hu, Z.; Han, C. C. *Angew. Chem.* **2003**, *115*, 4333.
(15) Liang, Z.; Susha, A. S. *Chem. Eur. J.* **2004**, *10*, 4910.

10.1021/cm0501564 CCC: $30.25 © 2005 American Chemical Society
Published on Web 07/09/2005

largely determined by the restructuring of cooperative assemblies between silica species and surfactant molecules. This method enriches the preparation techniques of mesoporous materials whether in theory study or application research.

β-Cyclodextrin is a cyclic oligosaccharide, and the inner surface of its toroidal cavity is hydrophobic while the exterior surface is hydrophilic,[16] which makes β-cyclodextrins an important rigid molecular receptor. Triton X-100 (TX-100) is a well-defined nonionic surfactant that is easily separated, nontoxic, biodegradable, and relatively inexpensive. Polarz et al. were the first to use cyclodextrines as template to create a wormlike mesoporous silica structure.[17] The supramolecular assemblies of β-cyclodextrins with nonionic surfactants such as Triton X-405 are used as templates in the strong acid condition by the nanocasting process for the generation of silica materials. The product mesoporous materials with wormholelike porous structures have better thermal stability.[16,18]

Experimental Section

Synthesis. β-Cyclodextrin (analytical grade, China Medicine Co.), Triton X-100 (99% purity, Amresco Co.), and TEOS (chemical grade, Tianjin Chemical Co.) were used without further purification. In a typical synthesis, 0.01 mol (1.135 g) of β-cyclodextrin was first added to 1.67 mol (30 g) of distilled water in a Teflon container, and then the mixture was heated and stirred until the β-cyclodextrin was dissolved completely. After cooling, hydrochloric acid was added to adjust the pH to 2.0. Then 1.6 g of TX-100 was added, and the mixture was stirred for 8 h. Next, 0.023 mol (4.8 g) of TEOS was added dropwise, and then the mixture stirred for 2 h. The precursor solution was poured into a 15.0 cm^3 stainless steel autoclave with a Teflon liner until 70% of the volume of the autoclave was occupied. After hydrothermal treatment at 100 °C for 12 h, the autoclave was cooled to room temperature, and the solid product was recovered by filtration, washed with distilled water, and dried at 100 °C for 2 h. The obtained products were calcined in an air-atmosphere tube furnace at a rate of 1 °C·min^{-1} from room temperature to 550 °C. After calcining at 550 °C for 5 h to completely eliminate the remaining surfactant molecules in the pores, the final product was cooled to room temperature in the furnace.

Characterization. X-ray diffraction (XRD) patterns of the as-synthesized and calcined samples were recorded on an X-ray diffractometer (Rigaku D/Max 2200PC) with a graphite monochromator and Cu Kα radiation ($\lambda = 0.15148$ nm) in the range of 1−10° at room temperature while the voltage and electric current were held at 28 kV and 20 mA. Thermal gravimetric (TG) analysis (TGA/SDTA, 851^{e}METTLER) at a rate of 20 mL/min in O_2 flow and heating rate of 20 °C/min was employed to measure the weight loss of samples. The surface morphology and diameter of microtubules were observed using a scanning electron microscopy (SEM, Hitachi S-520, JXA-840). A transmission electron microscope (TEM, Model H-800) and high-resolution TEM (HRTEM, GEOL-2010) were applied to observe the cross section and the internal structure of the microtubules. To further verify the morphological characteristics and ascertain the internal pore architecture of the microtubules, the samples were microtomed into thin slices and transferred onto bare copper grids for TEM observations. Nitrogen adsorption−desorption data were measured with an ASAP 2010 micromeritics apparatus at liquid nitrogen temperature ($T = -196$ °C). Isotherms were evaluated with the Barrett−Joyner−Halenda (BJH) theory to give the pore parameters, including surface areas, pore size, and pore distribution.

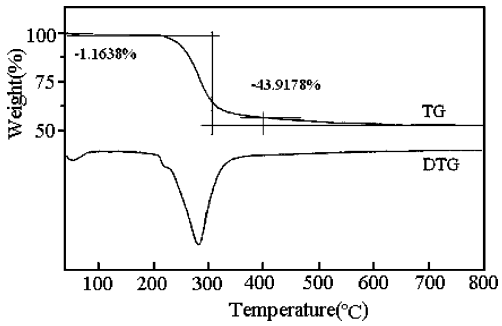

Figure 1. TG and DTG curves of microtubules subjected to hydrothermal treatment.

Results and Discussion

Hierarchically Structural Feature of Microtubules. The TG curve shown in Figure 1 indicates that the total weight loss of microtubules after hydrothermal treatment amounts to 45%. This includes three weight losses: the weight loss from 40 to 100 °C is due to the desorption of water, the significant weight loss of ca. 43% between 220 and 400 °C is caused by the decomposition of the organic template in the nanochannels of microtubule walls or the dissociative surfactant, and that above 400 °C is attributed only to the loss of water via condensation of silanol groups in the silica framework. In the third stage, siloxane bonds are formed and the weight loss is very small.[19] On the basis of the thermal analysis, a slow heating rate of 1 °C/min up to 550 °C with a hold time of 5 h is expected to drive off the template molecules gradually and completely.

The amorphous characteristics of the pore walls are evident in the X-ray reflection centered at $2\theta = 22-23°$, and the low angle XRD patterns of the hydrothermal and calcined samples are shown in Figure 2. The sample subjected to the hydrothermal treatment shows a broad diffraction peak centered at $2\theta = 1.6°$ corresponding to $d = 5.3$ nm (Figure 2a), and the sample calcined at 550 °C has a peak at $2\theta = 1.7°$ corresponding to $d = 5.1$ nm (Figure 2b). The diffractograms exhibit only a broad peak arising from the average pore-to-pore separation in the disordered wormhole framework, indicating that the arrangement of mesoporous channels in the microtubular walls is random.[20] The formation of silica structures occurred via a neutral-template route, in which an inorganic precursor, TEOS, is hydrolyzed to result in $Si(OC_2H_5)_{4-x}(OH)_x$ species, which evidently interact with the hydroxyl groups of the template molecules by hydrogen-bonding. Long-range effects of the electrostatic

(16) (a) Han, B.; Polarz, S.; Antonietti, M. *Chem. Mater.* **2001**, *13*, 3915. (b) Han, B.; Antonietti, M. *Chem. Mater.* **2002**, *14*, 3477.
(17) Polarz, S.; Smarsly, B.; Bronstein, L.; Antonietti, M. *Angew. Chem., Int. Ed.* **2001**, *40*, 4417.
(18) Han, B.; Smarsly, B.; Gruber, C.; Wenz, G. *Microporous Mesoporous Mater.* **2003**, *66*, 127.
(19) Newalkar, B. L.; Komarneti, S. *Chem. Mater.* **2001**, *13*, 4573.
(20) (a) Blin, J. L.; Léonard, A.; Su, B. L. *J. Phys. Chem. B* **2001**, *105*, 6070. (b) Gross, A. F.; Le, V. H.; Kirsch, B. L.; Riley, A. E.; Tolbert, S. H. *Chem. Mater.* **2001**, *13*, 3571. (c) Yuan, Z.; Ren, T.; Su, B. *Adv. Mater.* **2003**, *15*, 1462.

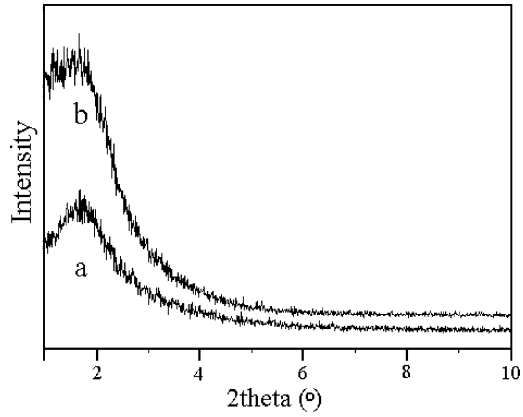

Figure 2. Small-angle XRD patterns of microtubules (a) subjected to hydrothermal treatment and (b) calcined at 550 °C for 5 h.

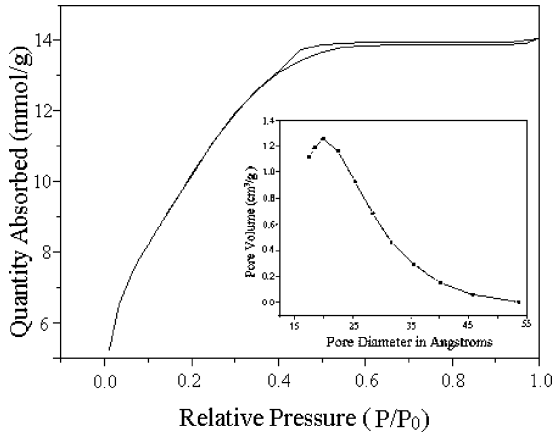

Figure 3. N_2 adsorption and desorption isotherms and the corresponding BJH pore size distribution curve (inset) at −196 °C for the sample obtained after calcination in air at 550 °C for 5 h.

interactions are absent. The increase in peak intensity after calcination might be due to the greater scattering density contrast and reduced X-ray absorbance after surfactant and polymer removal, not the enhancement of pore ordering.

Further experiments were carried out to study the formation of the mesoporous structure. If β-cyclodextrin is used as the sole template molecule without TX-100, but other experiment conditions are the same as those in the typical experiment, the obtained sample is spherical in morphology and does not have a mesoporous structure. When TX-100 was only used as the sole template molecule without β-cyclodextrin, the morphology of the sample was also spherical, but the spherical particles were mesostructured. The pore size in this experiment was the same as that in the typical experiement, but the shape of the mesopores was found to be different from that of the microtubules. This demonstrates that the mesoporous structure of microtubules is dependent on the supramolecular assembly of β-cyclodextrin with nonionic surfactant TX-100, and the assemblies determine the shape of the mesopores.

The representative N_2 adsorption−desorption isotherms and the corresponding BJH (Barret−Joyner−Halenda) pore size distribution (PSD) curve (inset) for the mesoporous microtubules are given in Figure 3. A small hysteresis loop is observed, and it shows a type of IV-like isotherm with a relatively sharp increase in the absorbed volume of nitrogen at $P/P_0 = 0.4$, indicating the presence of mesopores in the

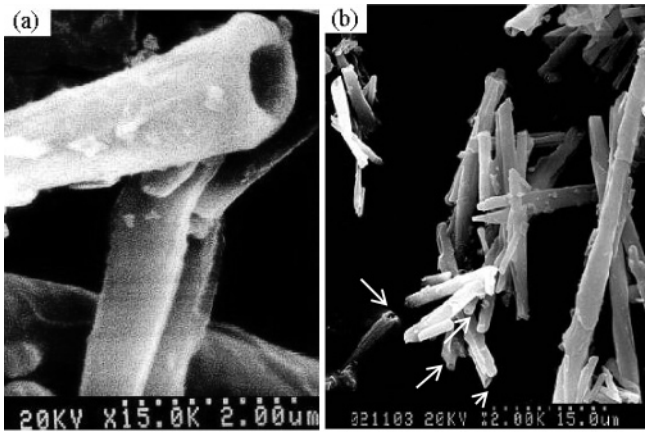

Figure 4. SEM images of the microtubules (a) subjected to hydrothermal treatment and (b) calcined at 550 °C for 5 h.

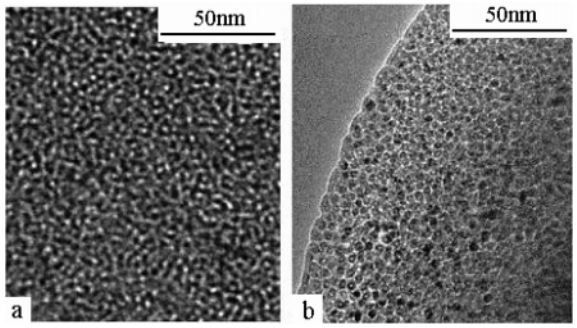

Figure 5. HRTEM images of microtubules calcined at 550 °C for 5 h. (a) HRTEM image of the wormholelike porous framework. (b) HRTEM image of the cross section of the mesopores. Each ring is a cross-section of the mesopores.

walls of microtubules. The BJH analyses show that the sample has a narrow pore size distribution and a pore size of ca. 2.3 nm. The Brunauer−Emmett−Teller (BET) surface area of the calcined mesoporous microtubules is 847 m^2/g and the maximum pore volume at $P/P_0 = 0.4$ by Horvath−Kawazoe is 0.45 cm^3/g. In view of the difference between d spacing (∼5.0 nm) and the pore diameter (2.3 nm), it is concluded that the microtubules have thick walls between the mesoporous channels.

The silica microtubules with few defects shown in Figure 4 are hollow with opened edges. The hierarchically structured microtubules (Figure 4a) derived from hydrothermal treatment exhibit a well-developed tubular morphology of 10−25 μm in length, 0.8−2 μm in diameter, and 0.3−1 μm in wall thickness. Comparing SEM images taken before and after calcination, the microtubules (Figure 4b) have no difference in morphology. The outer surface of the tubules appears relatively smooth, and the tubules still retain their tubular form without cracking, even after calcination (denoted by the arrows). Both ends of each tubule are open with a uniform shape.

The HRTEM images in Figure 5 show the internal architecture of the microtubules, channel architecture, and the hierarchical structure of a single hollow microtubule. The microtubules exhibit a 3D wormholelike porous framework and the wall thickness between mesoporous channels is ca. 2 nm (Figure 5a), which is in agreement with the low-angle XRD patterns. The wormholelike channel motif is a potentially important structural feature for favorable catalytic

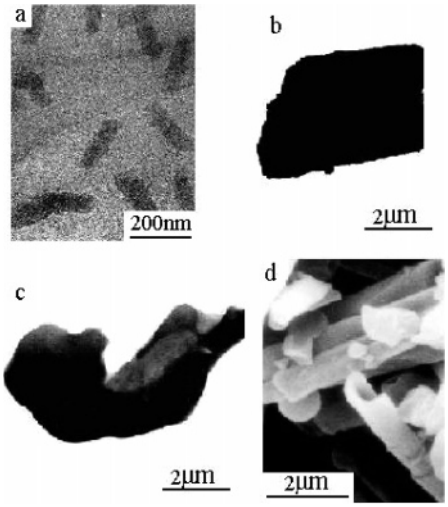

Figure 6. TEM images of (a) the surfactant/silica hybrid aggregates, (b) a patch of surfactant/silica composite aggregates, and (c) a bending patch in the hydrothermal process and an SEM image of (d) the coexistence of bending patches and microtubules.

reactivity, because channel branching within the framework can facilitate access to reactive sites on the framework walls and is expected to enhance the diffusion rate of reacting species, also it does not require any specific orientation for the design of filtration layers.[20−23] The pore topologies, i.e. the short tubelike morphology of pores forming the walls of microtubules, is observed (Figure 5b), which is consistent with the literature.[16] Each ring is the cross-section of the mesopores and the diameter is less than 2 nm. The short tubelike pore structures of silica materials definitely stem from the replication of the cylindrical shape of pseudopolyrotaxane, which is different from those of silica materials prepared by other structure-directing agents.[13,19] The hierarchical tubules-within-a-tubule structure and tubular nanochannels formed in the walls of microtubules are important for their technological promise in applications such as catalysis, selective separations, sensor arrays, waveguides, miniaturized electronic and magnetic devices, and photonic crystals with tunable band gaps.[22] In addition, they could act as minireactors and would have potential applications in nanotechnology.

Formation Mechanism of Microtubules. The precursor solution was stirred continuously for 24 h to produce the white surfactant/silica hybrid product. The hybrid product was filtered and washed with distilled water and then dried at 100 °C for 2 h. The morphology of surfactant/silica hybrid aggregates is club-shaped hybrid objects ca. 200 nm in length and ca. 50 nm in diameter (Figure 6a). In previous reports, much work focused on the self-assembled supramolecular structures based on nonionic surfactants including TX-100 and cyclodextrins, and the structure of the self-assembly (Supporting Information Figure S-4) was also confirmed by fluorescence, NMR, and TG analyses.[16,24−26] Thus, the hybrid objects are produced by the interaction between silica oligomers $Si(OC_2H_5)_{4-x}(OH)_x$ and the supramolecular assemblies of β-cyclodextrin with TX-100 by hydrogen-bonding at this step.[27] In the pH range 1−2, close to the isoelectric point of silica, the hydrolysis of TEOS is fast, whereas the condensation is slow.[28] Therefore, TEOS is quickly hydrolyzed in water at pH 1−2, producing stable small oligomers $Si(OC_2H_5)_{4-x}(OH)_x$. When TEOS is added to the surfactant solution, the species undergo spontaneous condensation and cooperative assembly at the molecular level forms the surfactant/silica composite aggregates.[21] After the precursor solution is treated at 100 °C for 4 h, the patches of surfactant/silica composite aggregates are observed (Figure 6b). The surfactant/silica hybrid aggregates are enlarged in area and thickness in the hydrothermal process, and the bending patches are produced as the time increases (Figure 6c). Some mesoporous silica microtubules form until the reaction time reaches 8 h (Figure 6d), and the bending patches and microtubules coexist in the product. The above results clearly support the view that the formation of the hollow structure occurs by an anisotropic membrane-to-tubule transformation. The formation of silica structures occurs via a neutral-template route. The driving force for bending arises from the random perturbation during the hydrothermal treatment. Therefore, the hydrothermal treatment process can drastically influence not only the regular organization of compounds on the nanometer scale but also their morphogenesis at the micrometer level.[29]

Figure 7 shows the FT-IR spectra of surfactant/silica hybrid aggregates and microtubules. The peaks around 800 and 1150−1050 cm^{-1} are related to the symmetric vibration and asymmetric vibration of Si−O−Si in SiO_4 tetrahedra.[21] The peak at 460 cm^{-1} (Si−O bending mode) is typical for silica materials, and the peak at 965 cm^{-1} is attributed to the symmetric stretching vibration of the Si−OH headgroup. The presence of water is supported by the appearance of the bending mode of water (δH_2O) at 1648 cm^{-1}, and the band at 3456 cm^{-1}, assigned to surface hydroxylation OH stretching mode of the framework Si−O−H, demonstrates that the surface of the porous channel is weakly acidic. But the broad peaks around 1100 and 2950 cm^{-1} consist of several small peaks (denoted by the arrows) that are the congruence of the absorption peaks of TX-100 surfactant and β-cyclodextrin. This indicates the presence of TX-100 and β-cyclodextrin in the samples after hydrothermal treatment. No significant shift can be observed from the IR spectrum of the surfactant/silica hybrid aggregates compared to TX-100 and β-cyclodextrin due to the serious overlap of the adsorptions, although the self-assemblies are formed at this step. The short tubelike pore structure of the surfactant/silica hybrid aggregates replicates the structure of the original supramolecular template of TX-100 and β-cyclodextrin. As a polyhydroxy oligosaccharide, β-cyclodextrin plays an essential role in the

(21) Boissière, C.; Larbot, A.; Lee, A.; Kooyman, P. J.; Prouzet, E. *Chem. Mater.* **2000**, *12*, 2902.
(22) Yang, P.; Deng, T.; Zhao, D. Y.; Feng, P.; Pine, D.; Chmelka, B. F.; Whitesides, G. M.; Stucky, G. D. *Science* **1998**, *282*, 2244.
(23) Xu, A. *J. Phys Chem. B* **2002**, *106*, 13161.
(24) Topchieva, I.; Karezin, K. *J. Collids Interface Sci.* **1999**, *213*, 29.
(25) Harada, A.; Li, J.; Kamachi, M. *Macromolecular* **1993**, *26*, 5698.
(26) Datta, A.; Mandal, D.; Pal, S. K.; Das, S.; Bhattacharyya, K. *J. Chem. Soc., Farady Trans.* **1998**, *94*, 3471.
(27) Boissière, C.; Larbot, A.; Bourgaux, C.; Prouzet, E.; Bunton, C. A. *Chem. Mater.* **2001**, *13*, 3580.
(28) Brinker, C. J. *J. Non-Cryst. Solids* **1988**, *100*, 31.
(29) Léonard, A.; Blin, J. L.; Robert, M.; Jacobs, P. A.; Cheetham, A. K.; Su, B. L. *Langmuir* **2003**, *19*, 5484.

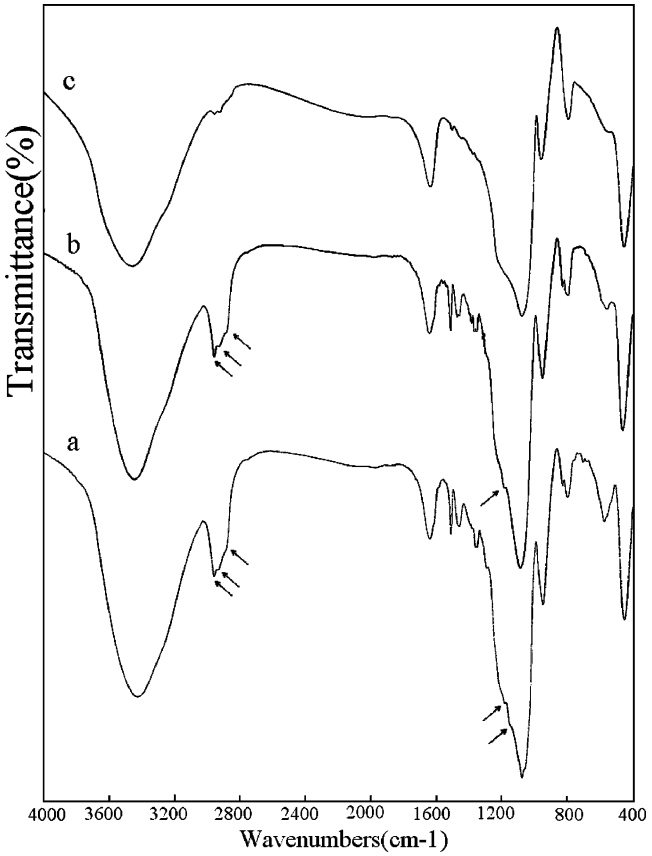

Figure 7. FT-IR spectra of (a) surfactant/silica hybrid aggregate, (b) the hydrothermal treated sample, and (c) the sample calcined at 550 °C for 5 h.

formation of hybrid objects, the pseudopolyrotaxanes, with silica species by H-bonding. The effects of H-bondings are the main reason for the formation of the patches, which is dependent on the pseudopolyrotaxanes of β-cyclodextrin with TX-100. Furthermore, β-cyclodextrin was shown to be present in both of the surfactant/silica hybrid aggregates and the hydrothermal product through FT-IR analysis. Thus the tubular morphology of products obviously contrasted to that of the spherical product formed without β-cyclodextrin or TX-100.

A small quantity of folded sheet, helical ribbons, incomplete tubules, and double-layered microtubules was also collected, and all were comprised of the same wormholelike mesoporous silica (Supporting Information Figure S-1-2). From the collective evidence we now propose the possible formation process of mesoporous silica microtubules, namely, a membrane-to-tubule transformation that arises from the moment perturbation effects the hydrothermal process, summarized in Figure 8. The bending direction is parallel to the axis of pseudopolyrotaxanes. In our synthetic system, the precursor solution is subjected to the hydrothermal environment, and the assembly of inorganic precursors around the template molecule is random and occurs through H-bonding (Figure 8A−C). In general, most of these hierarchical structures, and in particular the large-scale morphologies, are synthesized under acidic conditions through weak hydrogen-bonding forces.[9] As the patch grows in various dimensions, bending occurs in the direction parallel to the axis of pseudopolyrotaxanes, and the folded patch is

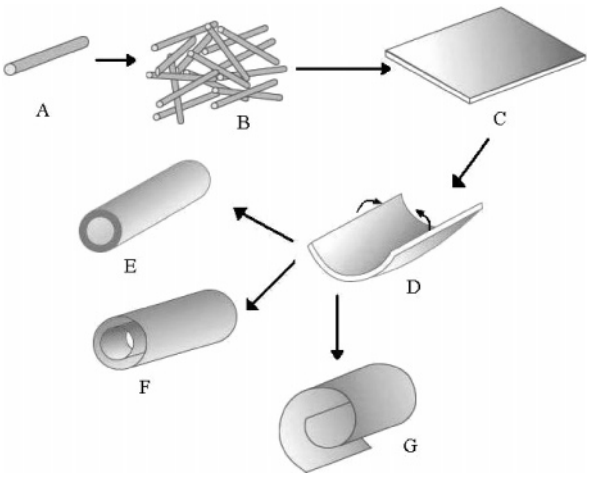

Figure 8. Proposed formation mechanism of microtubules: (A, B) random pseudopolyrotaxanes of β-cyclodextrin with TX-100 formed by H-bonding, (C) a patch of aggregates containing pseudopolyrotaxanes and hydrolyzed TEOS, (D) the enlarged patch bending in the hydrothermal process, (E, F) single and double-walled silica microtubules, and (G) helical ribbons.

considered to be stress-free. The random perturbation effects lead to patch bending during the hydrothermal process (Figure 8D). Unbalanced energy makes the metastable patch bend during the hydrothermal process. The thickness of the patches is inhomogeneous, and H-bonding interactions also exist among the patches. The thick patch is likely a splice of two or several patches. It can be seen that the wall thickness of microtubules from SEM and TEM images varies from less than 200 nm to 1 μm, due to the different thickness of patches, and the thicker membrane favors forming the single layer microtubule. Double-layered microtubules might form through the bending of two thinner patches (Figure 8E,F). If the bending direction is not balanced, a helical ribbon will be formed (Figure 8G). There into, single-walled microtubules account for the majority; next are double-walled products, and a small amount of helical ribbons is produced. The energy is unbalanced in the different parts of the autoclave in the hydrothermal process, and the drive force of patch bending is random perturbation, so the most likely products are E. If the random perturbation happens in two thin patches, the double-layered microtubules will form.

To further confirm the effect of the cooperation between cyclodextrins and TX-100 on the formation of the microtubules, another experiment is carried out, in which β-cyclodextrins is replaced by α-cyclodextrins, and other experiment conditions are the same as those in the typical experiment. Although the yield of the mesoporous silica microtubules is low, the mesoporous silica microtubules also can be obtained (Supporting Information Figure S-3). The result reveals that the cooperation between cyclodextrins and TX-100 is crucial in the formation of microtubular morphology from the other point.

Conclusions

In conclusion, the mesoporous silica microtubules are synthesized by a simple one-phase route via hydrothermal treatment. Supramolecular assemblies of β-cyclodextrins with the nonionic surfactant Triton X-100 are used as structure-directing agents in aqueous solution. This method enriches

the preparation techniques of mesoporous materials for theoretical study and applied research. The silica microtubules have a hierarchical organization of tubules-within-a-tubule, which forms the walls of the microtubules, and the short tubelike morphology of pores is observed. The microtubules exhibit a 3D wormholelike porous framework, and the thickness of walls between the mesoporous channels is ca. 2 nm. The formation mechanism is based on the bending of the mesoporous silica membrane, where the random perturbation effects lead to the patch bending in the hydrothermal process.

Supporting Information Available: HRTEM and SEM images of microtubules and a diagram of the pseudopolyrotaxanes (PDF). This material is available free of charge via the Internet at http://pubs.acs.org.

CM0501564